Analysis of Old Copper Synchrotron Light Absorbers from the Stanford Positron Electron Accelerating Ring

Sara R Marshall

Office of Science, SULI Program

Franklin W. Olin College of Engineering

Stanford Linear Accelerator Center

Menlo Park, California

August 3, 2005

Prepared in partial fulfillment of the requirements of the Office of Science, U.S. Department of Energy Science Undergraduate Laboratory Internship (SULI) Program under the direction of Benjamin Scott in Accelerator Systems Development Engineering & Technology Services of the Stanford Synchrotron Radiation Laboratory at the Stanford Linear Accelerator Center.

Participant: _____
Signature

Research Advisor: _____
Signature

Work supported by Department of Energy contract DE-AC02-76SF00515

Table of Contents

Tables

Figures

Abstract

Analysis of Old Copper Synchrotron Light Absorbers from the Stanford Positron Electron Accelerating Ring. SARA MARSHALL (Olin College of Engineering, Needham, MA 02492) BEN SCOTT (Stanford Linear Accelerator Center, Menlo Park, CA 94025).

Synchrotron light absorbers intercept synchrotron radiation to protect chamber walls from excessive heat. When subjected to the high temperature of the beam, these absorbers undergo thermal stress. If the stress is too great or fatigues the material, the absorbers may fail. These absorbers are designed to last the lifetime of the machine. Any premature cracking could result in a leak and, consequently, loss of the ultra high vacuum environment. Using secondary and backscattered electron techniques, several sections of a used copper absorber were analyzed for material damage. Chemical analyses were performed on these samples as well. Comparing the unexposed sections to the sections exposed to the electron beam, few cracks were seen in the copper. However, the exposed samples showed heavy surface damage, in addition to crevices that could eventually result in material failure. Significant corrosion was also evident along the water cooling passage of the samples. These findings suggest that further investigation and periodic inspection of absorbers in SPEAR3 are necessary to control corrosion of the copper.

INTRODUCTION

Synchrotron light absorbers protect the beam chamber walls from excessive heat due to the radiation given off by the accelerated beam. Some of these absorbers use oxygen free electronic (OFE) grade copper tubes, cooled with water, to mask the beam section walls. The current design practice is to limit the thermal stress in these absorbers to less than the fatigue strength of copper. Any cracks along the grain boundaries jeopardize the performance of the copper and may cause a catastrophic water leak into the high vacuum environment. Copper has no defined fatigue limit; any number of cycles could damage the structure. So, in practice, this means that many absorbers employ GLIDCOP, a dispersion hardened alloy, as the primary heat conducting material because of the high yield strength.

In this investigation, the absorber used in Beam Line 10 (BL10) of the second Stanford Positron Electron Accelerating Ring (SPEAR2) for 16 years was analyzed to determine whether the absorbers experienced any critical damage. The analysis included the observation of select sections of the copper tubing (see Figure 1) under the scanning electron microscope (SEM), using secondary (SE) and back-scattered (BE) electron techniques to search for material damage due to continuous thermal stress. In addition, energy dispersive x-ray spectrometry (EDS) was used to analyze material compositional changes. Using this technology, the properties of new copper were compared to the property data of the fatigued copper. Absorbers from BL11 were also observed to provide additional evidence for corrosion. The properties of each absorber are listed in

Table 1, some of the values of which were taken from a previous study [1]. Further investigation could shed light on the mechanical situation of the copper absorbers.

MATERIALS AND METHODS

All samples were OFE copper taken from the SPEAR2 storage ring. Using a low stress-inducing water-cooled Buehler Abrasimet 2 diamond blade saw, six samples were cut from one absorber: 2 control cross-sections, 1 control surface, 2 experimental cross-sections, and 1 experimental surface. The control samples were taken from the part of the absorber that was not exposed to the electron beam. The experimental samples were taken from the exposed part (see Figure 1).

After cutting, the samples were mounted in 25 cubic centimeters of Buehler transoptic powder using a Simplimet 3 mounting press in preload mode. The resin mount allows for easier observation of the samples. The press operated for 5.5 minutes with a temperature of 150°C and a pressure of 3900psi.

Each sample was prepared for analysis according to ASTM standard E3 [2]. This allows for uniform sample preparation. Rough grinding was done using a Power Pro 5000 water cooled system with Buehler metallurgical grade silicon carbide paper at 150 reps per minute (RPM) for 40 second intervals. Paper was replaced after each cycle. The grit sizes used and their respective repetitions are listed in Table 2.

After grinding, the samples were coarsely polished using a Power Pro 5000 system with Struers diamond suspension in 6µm, 3µm and 1µm sizes at 120 RPM. Samples ran once for each size. Nylon 1000 cloth loaded with ¾ gram of Buehler Metadi

paste was used for the 6µm run for 5 minutes. Struers MOL woven wool cloth loaded with Metadi paste was used for the 3µm interval for 4 minutes. Buehler Microcloth synthetic cloth was used for the 1µm run for 3.5 minutes.

Each sample was finish-polished using a Power Pro 5000 system with Struers 0.06µm OP-S colloidal silica suspension on an OP-CHEM porous neoprene cloth surface for 3 minutes at 100 RPM.

Vibratory polish was used to remove fine scratches at a setting of 35. Using a Microcloth loaded with 150ml of 0.02µm Mastermet 2 non-crystallizing colloidal silica suspension, the samples were polished for 2.5 hours. The polishing procedure removed most of the surface scratches, leaving a few small ones behind.

Observation of the samples took place after the completion of polishing. Cross-sections were viewed using the optical microscope at magnifications ranging from 25 to 200x. The SEM was used to analyze the surface samples at magnifications ranging from 15 to 5000x. Chemical analysis was performed on the surface samples using EDS techniques.

The absorbers from BL11 were cut using a Buehler band saw. After deburring the edges of each cut, the sections were observed with a magnifying glass and then followed the same preparation procedure discussed above. Corrosion depth was estimated by using Vermont Gage Series C Plus gauges to measure the inner diameters of the tubing. The valleys of the corrosion ring were measured using electronic calipers from the gauge to the tip of the valley. Measurements taken from the cut samples are listed in Table 3.

RESULTS

The three observation techniques each gave a snapshot of the mechanical and thermal damage withstood by the absorber. The SE method showed extensive surface scratches on the control and the experimental samples (see Figure 2). At 1000x magnification, the experimental sample showed heavy grooves along the surface. Figure 3 compares the control sample surface to the experimental sample surface at this magnification.

Figure 4 displays the surface of each sample using the BE technique. The BE method constructs an image of the surface of a sample according to atomic number, as opposed to the SE method, which builds an image based on topography.

Table 4 shows the results of the chemical analysis. Each sample contained carbon and oxygen in addition to copper. The amount of carbon stayed around the same level; however the experimental sample showed greater amounts of oxygen than did the control.

The outer edge of each sample was observed using the optical microscope. Figure 5 illustrates the mechanical damage sustained by the sample exposed to the intensity of the electron beam.

Figure 6 displays the edge of the water cooling passage of the absorber. Each sample showed heavy indentation. The extent of this mechanical damage for each absorber is listed in Table 3. Figure 7 shows the overall cross-section of the experimental sample.

Using the optical microscope, grain structure was observed. Figure 8 illustrates the effect of heating on water-cooled OFE copper. The experimental sample sustained substantial grain growth and thus thermal damage.

Table 1 lists the properties of each absorber. Values noted with * were taken from a previous study [1]. Thermal stress data was determined by using a two-dimensional ANSYS model. Flow velocity was calculated by dividing the flow rate by the area of the cross-section of the water passage ($v = \frac{q}{A}$).

The corrosion depth and diameter of Table 3 were measured using the procedure discussed in *Materials and Methods*.

Figure 9 illustrates the plating discovered on the inner surface of the BL10 near absorber. Plating of this type was found on each absorber studied.

DISCUSSION AND CONCLUSION

In order for OFE copper to fail, extensive grain movement must occur. When individual grains move within a material, they push into each other. Often the force causes the grains to slip and pull apart from one another. This movement results in the cracks characteristic of failure. When intense heat is added to the system, the grains begin to fuse together, leaving behind larger and fewer grains. This grain growth weakens the material as there are fewer grains to support the structure. The investigation of the BL10 absorber showed evidence of high grain activity. Comparing the control to the experimental sample in Figure 3, it is clear that the structure of the copper changed during its exposure to the electron beam.

Despite the surface scratches, distinct grooves can be seen in the experimental sample (see Figure 5). These features could be deeper surface scratches, or could be the result of grain separation. But since these grooves do not seem to occur along grain boundaries, they may be deeper surface scratches.

The experimental sample experienced substantial grain growth during its time in operation, as evidenced by Figure 8. As copper is formed into a tube, grains break up, leaving vast amounts of small grains. As a result of this work-hardening, the material strengthens. Heat undoes this hardening, fusing grains together.

An unexpected result of the absorber usage was the significant corrosion experienced by the inner surface of the tube. This corrosion could be the result of fast flowing or stagnant water. According to an outside study [3], when oxides form on the copper surface and carbon dioxide is present in the water, the CO_2 forms an acid that breaks down into hydrogen atoms and HCO_3^-. The hydrogen atoms react with the oxygen atoms on the surface of the copper to form water. The copper dissolves and the process continues. In addition, the water flowing through the far BL10 tube ran with a velocity of 22.1 ft/s. Typically, the flow velocity is set at 15 ft/s to provide a high heat transfer coefficient and reduced cavitation. The velocities experienced by these absorbers fall in the undesired range. At these speeds, the copper tends to corrode at a faster rate than a normal absorber.

Interestingly, the absorbers from BL10 and 11 appear to have material deposited inside the tubes. Before use, the BL11 absorbers were gun-bored with a 0.25” diameter. As seen from Table 3, the diameters of these samples decreased, indicating that material was deposited and plated to the inside of the tube during use. This plating can be seen

along the inside of each tube (see Figure 9). The composition of the deposit was found to be copper oxide. An EDS test performed on the inner surface showed high levels of oxygen and copper. This indicates that the high velocity of the water forced some of the corroded material onto the walls of the water passage.

One way to prevent the copper from severely corroding would be to slowly circulate the water through the absorbers during shutdown periods. This would help prevent stagnation. Another way would be to keep the velocities of the water at reasonable levels during each run. Taking an unused SPEAR3 absorber and subjecting it to controlled high flow velocities as well as stagnant water would provide additional information as to the severity of these problems under optimal operating conditions.

This research has provided valuable information concerning the effects of high temperatures on the synchrotron light absorbers used in the SPEAR storage ring. With this knowledge of corrosion and material weakening, the engineers of the Stanford Synchrotron Radiation Laboratory can take greater steps to prevent catastrophic failure in the future.

ACKNOWLEDGEMENTS

This research was conducted at the Stanford Linear Accelerator Center. I would like to thank my mentor Ben Scott for his knowledge and support. Also I thank my colleagues Rebecca Armenta and Matthew Crockett for their enthusiasm and input. Many thanks go to Bob Kirby, Will Glesener, and Mike Swanson for preparing the samples. I also thank Stacey Block for her support. Finally, I would like to extend my

gratitude to the U.S. Department of Energy, Office of Science for granting me the opportunity to participate in the exceptional SULI Program and the chance to have an exciting internship.

REFERENCES

[1] Ross, Max, *Synchrotron Radiation Mask Temperature and Stress Results and Analysis: SPEAR2 Masks in the Beam Line 5, 9, 10, 11 Insertion Device Vacuum Chambers*, SSRL Engineering Note M485, 2004.

[2] ASTM E3: Standard Methods of Preparation of Metallographic Specimens.

[3] Dortwegt, R., "Low-Conductivity Water Systems for Accelerators," *2003 IEEE Particle Accelerator Conference*, pp 630-634, 2003.

TABLES

Absorber	Service Length (yrs)	Material	Power input* (watt/cm)	ΔT metal/metal-water interface* (°C)	LCW velocity (ft/sec)	Thermal Stress* (ksi)
BL10 far	16 run cycles Inst 87 Rem 04	OFE Cu	78.9	27.1/57.9	*13.5gpm* 22.0	11.5
BL10 near		OFE Cu	46.6	19.2/35.2		8.1
BL11 far	5 run cycles Inst 98 Rem 04	OFE Cu	59.0	31.4/126.9	*4.7gpm* 30.9	13.3
BL11 mid		OFE Cu	47.9	28.0/106.7		11.8
BL11 near		OFE Cu	62.6	40.8/144.4		17.3

Table 1: Properties of each absorber observed. Each value corresponds to the maximum current experienced by these absorbers (200mA). Inst stands for installed, Rem stands for removed. * Taken from previous study [1].

Grit	# of Repetitions
320	3
400	3
600	5
800	5

Table 2: Number of times samples were run for each grit size.

Absorber	Corrosion Depth (in)	Original Diameter* (in)	Measured Diameter (in)
BL10 far	0.018	0.5[#]	0.462
BL10 near	0.018	0.5[#]	0.475
BL11 far	0.017	0.25	0.227
BL11 mid	0.008	0.25	0.225
BL11 near	0.012	0.25	0.242

Table 3: Corrosion depths and diameters of the absorbers studied. *Original diameter taken from drawing. [#]Drawing not available, value is estimated.

Sample	Chemical Composition *(in order of abundance)*
Control	Cu, C, O, S
Experimental	Cu, O, S, C

Table 4: Chemical composition of each sample.

FIGURES

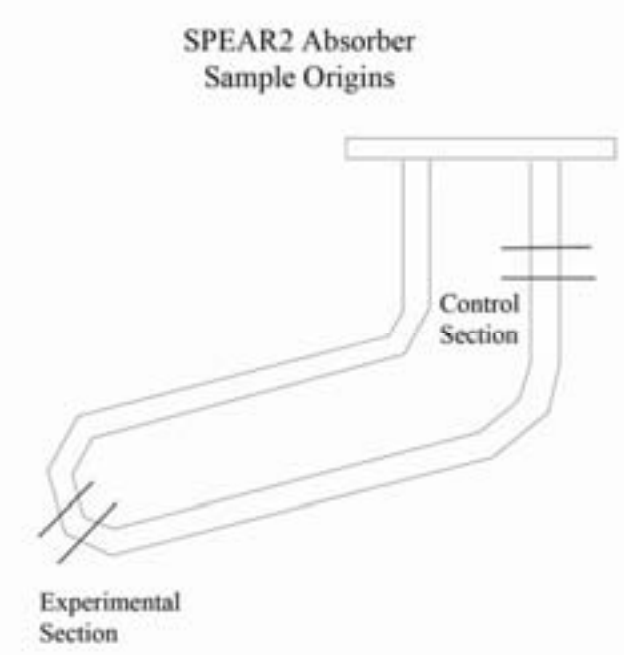

Figure 1: Image identifying original locations of samples.

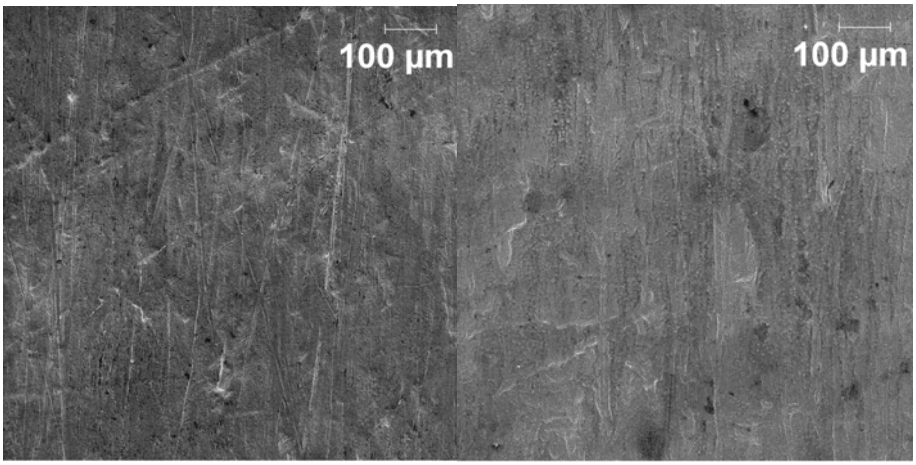

Figure 2: SEM image of surface scratches on both samples, control (left) and experimental (right) at 100x magnification

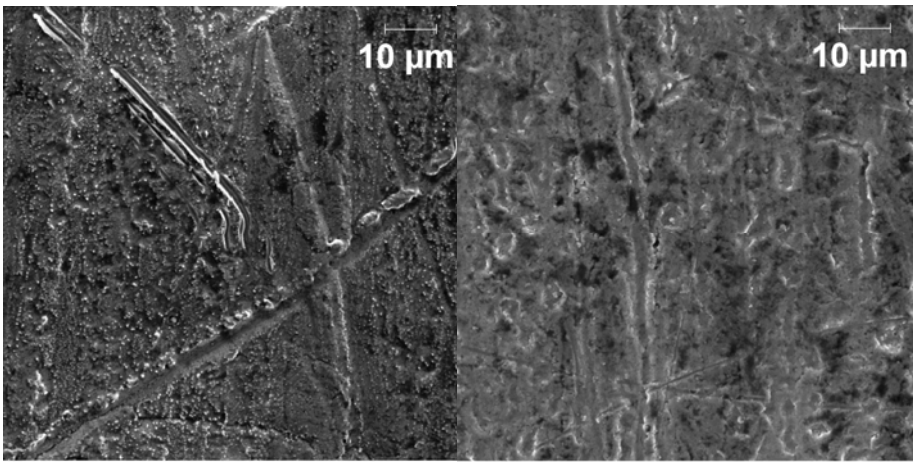

Figure 3: SEM image of outer surface of samples at 1000x magnification. Experimental (right) shows grain movement and structure change.

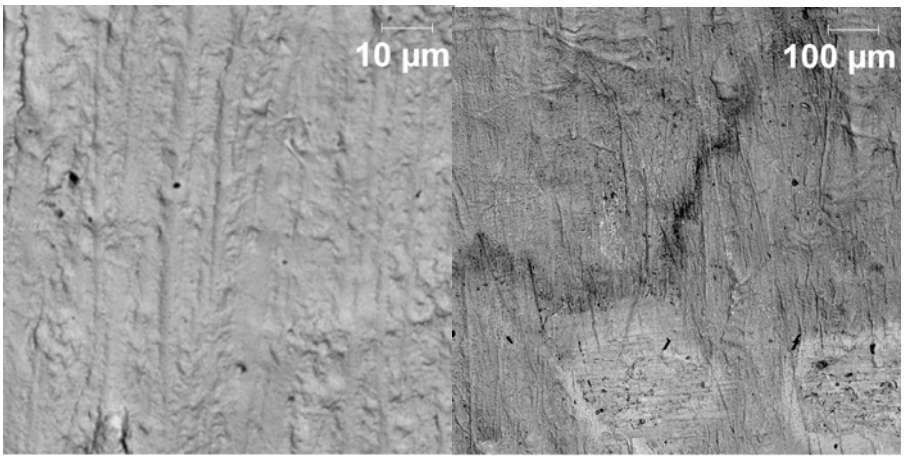

Figure 4: BE image of sample surfaces. Control (left) at 1000x magnification. Experimental (right) at 100x magnification. Experimental shows greater color change.

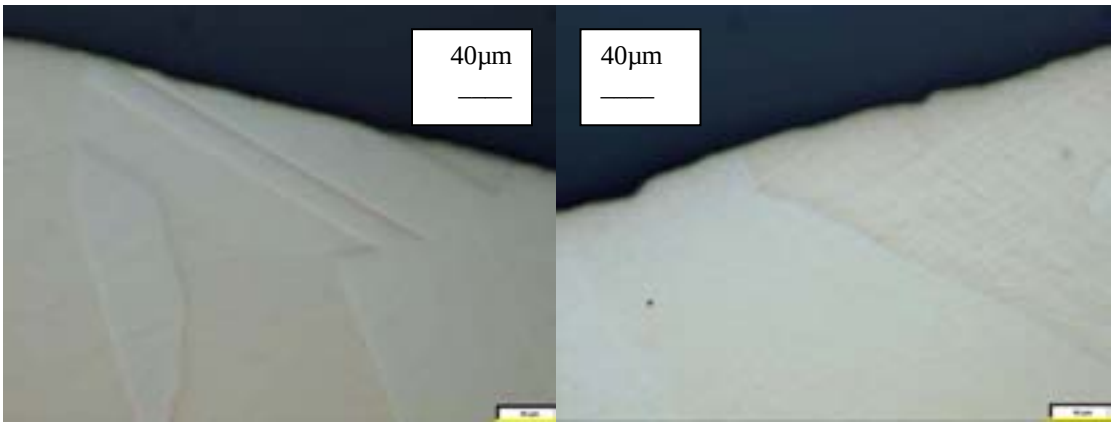

Figure 5: Outer edge of samples seen through optical microscope at 200x magnification. Control (left) shows a smoother edge than experimental (right).

Figure 6: Inner edge of absorber at 25x magnification showing water corrosion. The experimental (right) shows greater damage.

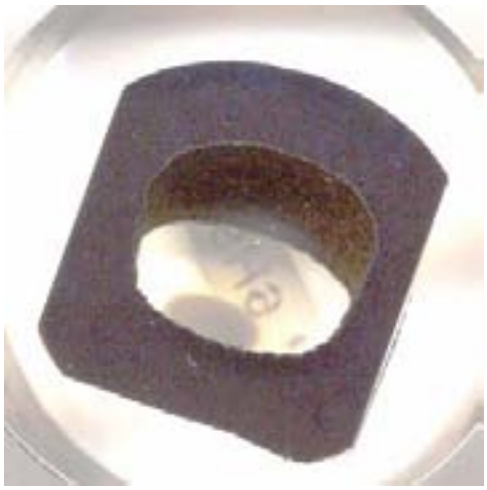

Figure 7: Cross-section of experimental sample. Corrosion is evident along the inner edge of the section. Figure 6 experimental sample enlarges this section. Image enlarged 2.5 times.

Figure 8: Grain structure of samples at 25x magnification. Control (left) has an overall smaller grain size than the experimental sample (right).

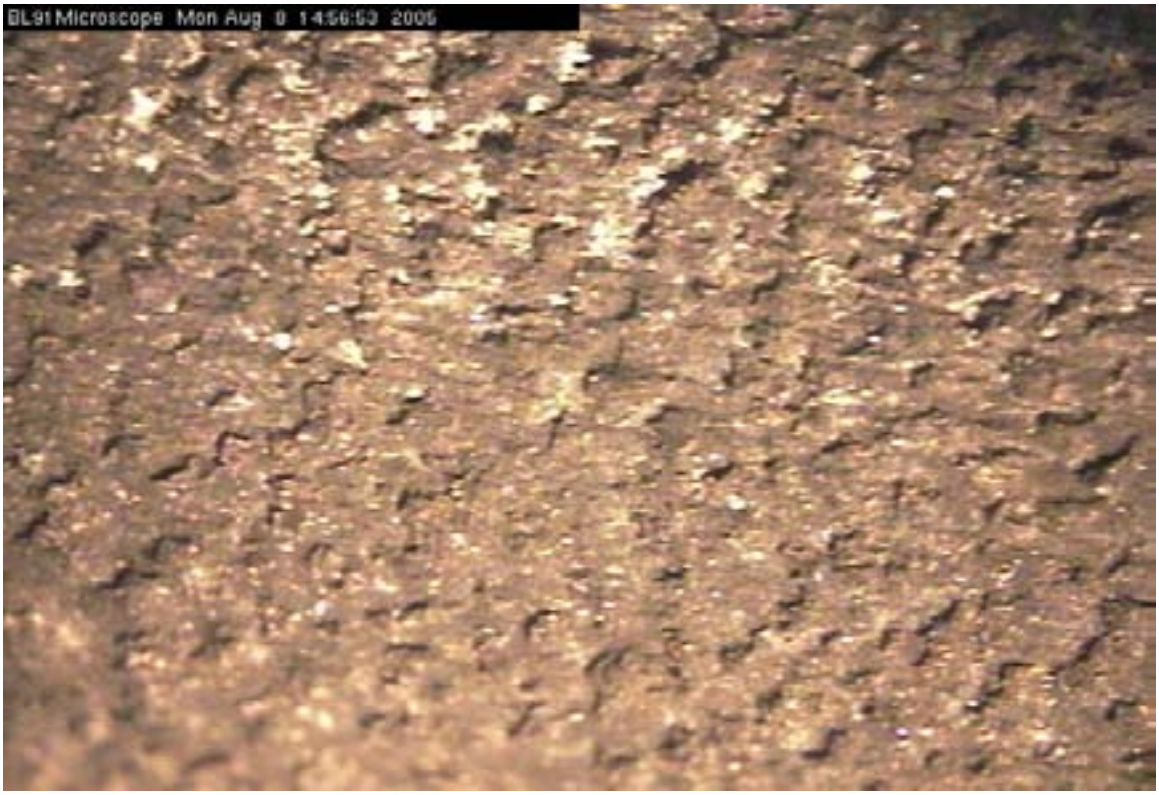

Figure 9: Image taken from BL9-1 microscope showing black deposit on water cooling passage, 12.5x magnification.